Original Article

Standard diffusion-weighted, diffusion kurtosis and intravoxel incoherent motion MR imaging of the whole placenta: a pilot study of volumetric analysis

Tao Lu[1], Yishuang Wang[1], Aiwen Guo[1], Cui Wei[1], Yazheng Chen[1], Shaoyu Wang[2], Bin Song[3]

[1]Department of Radiology, Sichuan Provincial People's Hospital, University of Electronic Science and Technology of China, Chengdu, China; [2]MR Scientific Marketing Specialist, Siemens Healthineer, Shanghai, China; [3]Department of Radiology, West China Hospital, Sichuan University, Chengdu, China

Contributions: (I) Conception and design: T Lu; (II) Administrative support: B Song; (III) Provision of study materials or patients: Y Wang, C Wei; (IV) Collection and assembly of data: A Guo, Y Chen; (V) Data analysis and interpretation: T Lu, S Wang; (VI) Manuscript writing: All authors; (VII) Final approval of manuscript: All authors.

Correspondence to: Bin Song. Department of Radiology, West China Hospital, Sichuan University, No. 37, Guoxuexiang, Chengdu 610037, China. Email: songb_radiology@163.com; Tao Lu. Department of Radiology, Sichuan Provincial People's Hospital, University of Electronic Science and Technology of China, No. 32 West Second Section, First Ring Road, Chengdu 610072, China. Email: 345248302@qq.com.

Background: Using magnetic resonance imaging (MRI) to explore the changes in microvascular perfusion fraction and the heterogeneity of the placenta during pregnancy.

Methods: We retrospectively reviewed 24 patients with normal pregnancies who underwent standard diffusion-weighted, diffusion kurtosis, and intravoxel incoherent motion MRI. The mean, minimum and maximum parameters including the apparent diffusion coefficient (ADC) and exponential ADC (eADC) from standard diffusion-weighted imaging (DWI), the diffusion coefficient (MD) and diffusion kurtosis (MK) from diffusion kurtosis imaging (DKI), and the pure diffusion coefficient (D), pseudo-diffusion coefficient (D*) and perfusion fraction (f) from intravoxel incoherent motion MR imaging (IVIM) were calculated from the whole placenta volumetric analysis and correlated with gestational age (GA) and volume of the placenta.

Results: A significant positive correlation was found between eADC mean, eADC max, MK mean, MK max, the volume of the whole placenta, and GA, and a negative correlation was found between ADC mean, ADC min, MD min, D mean, D min, D* min and GA. The f mean and MK max values positively correlated with the volume of the whole placenta.

Conclusions: eADC mean, eADC max, MK mean, MK max values increased with GA, while ADC mean, ADC min, MD min, D mean, D min, D* min decreased with GA. Secondly, the f mean and MK max also increased with placental volume. These results suggest the potential of diffusion and perfusion parameters to evaluate the placenta during its development using different DWI models.

Keywords: Diffusion kurtosis imaging (DKI); diffusion magnetic resonance imaging (diffusion MRI); intravoxel incoherent motion; magnetic resonance imaging; placenta

Submitted Feb 16, 2022. Accepted for publication Mar 16, 2022.
doi: 10.21037/atm-22-1037
View this article at: https://dx.doi.org/10.21037/atm-22-1037

Introduction

The placenta is a highly specialized organ that supports the continuing growth and development of the fetus and facilitates physiological exchange with the mother. The intervillous space is where the maternal and fetal circulations coincide, with the maternal blood bathing the villi and draining back through endometrial veins to ensure the necessary blood supply, efficient transfer of nutrients

and gases, and waste removal (1).

Changes in placental development and function can dramatically affect the fetus and result in a wide range of pregnancy complications, including pre-eclampsia, intrauterine growth restriction (IUGR), and abruption (2).

Ultrasound (US) is the firstline modality used during pregnancy, but it is limited in the evaluation of placental function and physiological characteristics. Magnetic resonance imaging (MRI) is a safe and complementary imaging modality to ultrasound, ensuring further evaluation of the placenta and the fetus with high-resolution and soft-tissue contrast, especially when the findings from US are equivocal. A growing number of studies have used functional MRI to monitor placental blood flow and function because it is a versatile technique that is free of ionizing radiation and exogeneous contrast agents (3-5).

Diffusion-weighted imaging (DWI), a method measuring the Brownian motion of water molecules and noninvasively evaluating tissue biophysical characteristics, is already routinely used in placental MRI (6-9). Conventional DWI is based on Gaussian diffusion behavior and follows a mono-exponential model. With the apparent diffusion coefficient (ADC), information on the microscopic motion of water protons is revealed. However, due to diffusion barriers, such as membranes and organelles, diffusion of water molecules in biological tissue is more confined and complicated (10). First proposed by Jensen *et al.*, diffusion kurtosis imaging (DKI) is a non-Gaussian diffusion-weighted model capable of describing the complicated water diffusivity in histological tissue and better reflects tissue heterogeneity and cellularity with high b-values (11). Recently, DKI has been adopted for the evaluation of tumors and neurological diseases (12-18). Intravoxel incoherent motion MR imaging (IVIM) is a bi-exponential model initially proposed by Le Bihan (19) that helps distinguish pure molecular diffusion from capillary perfusion when separating the fast perfusion-driven component from a slow diffusion-driven component. First introduced into placental MRI in the 2000s (20-22), IVIM is now widely used in the evaluation of placenta accreta spectrum disorders (PAS) disorders, placental insufficiency, and small for gestational age (GA) neonates (23-26).

The hybrid IVIM-DKI model is the combination of different diffusion models, namely IVIM and DKI. In recent years, it was developed from the increasing number of studies on the assessment of tumors (12,14,15,27,28). Because different tissue characteristics can be achieved with mono- and bi-exponential DWI and DKI, there may be value in investigating their roles in the evaluation of placental function.

The hybrid IVIM-DKI model has yet to be adopted in the evaluation of GA-related changes in tissue characteristics in the placenta. Previous volumetric analysis of placenta mainly studied the correlation between placental volume and change of gestational age (29). However, placental cellular heterogeneity and hemodynamic effects also change with the increasing gestational age. Therefore, the aim of this study was to demonstrate the feasibility of the hybrid model in the evaluation of perfusion, diffusion, and the microscopic structural complexity of the placenta during gestation. We present the following article in accordance with the MDAR reporting checklist (available at https://atm.amegroups.com/article/view/10.21037/atm-22-1037/rc).

Methods

Study population

The study was conducted in accordance with the Declaration of Helsinki (as revised in 2013). This study was approved by the institutional review board of Sichuan Provincial People's Hospital (approval No. 2021-282) and written informed consent was given by all participants. Patients with singleton pregnancies attending scans for underlying PAS disorders at 19–38 weeks between December 2018 and May 2020 were included in the study. All pregnancies were dated by US scan in the first trimester. Patients with placental abnormalities (n=42), inadequate surgical records (n=27), or severe artifact (n=2) were excluded. Patients with hypertension (n=2), pre-existing renal disease (n=1), diabetes mellitus (n=3), and claustrophobia (n=1) were also excluded (*Figure 1*). Data of pregnancy outcomes were obtained from maternity records or the patients' general practitioners. A normal pregnancy was defined as a healthy, singleton pregnant woman giving birth at term (≥37 weeks of gestation) to a newborn with appropriate weight for GA (birth weight within ±2 standard deviations of the Chinese reference standard for newborns) (30).

MR techniques

MRI examinations were performed with a 1.5-T MR scanner (Aera, Siemens Healthineers, Erlangen, Germany) using a 16-channel body coil. Besides routine MR sequences (HASTE, Tru-fisp, and T1WI) used for

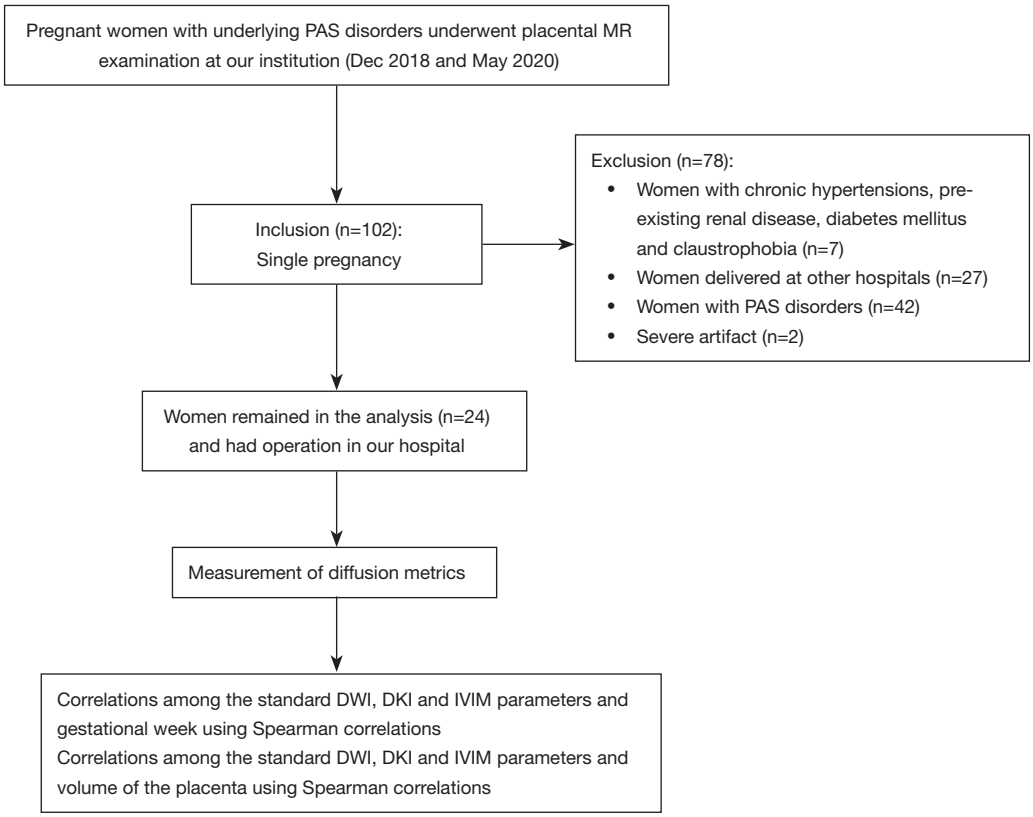

Figure 1 Flowchart of the study design. PAS, placenta accreta spectrum disorders; MR, magnetic resonance; DWI, diffusion-weighted imaging; DKI, diffusion kurtosis imaging; IVIM, intravoxel incoherent motion MR imaging.

placental MRI, single-shot echo planar imaging (EPI-DWI) was performed to obtain isotropic images with a pair of rectangular diffusion gradient pulses along all three orthogonal axes. The following imaging parameters were used: TR/TE: 5,200/83 ms, acquisition matrix: 192×120, field of view (FOV): 288×384 mm, number of averages: 2, slice thickness/intersection gap: 5 mm/1 mm and parallel imaging acceleration factor: 2. In addition, 11 different b-values (b=0, 50, 100, 150, 200, 400, 600, 800, 1,000, 1,200 and 1,600 s/mm^2) were applied. The total scan time for the DWI sequence was 7 min 29 s.

Imaging analysis

Standard mono-exponential DWI is expressed as (12):

$$Sb / S0 = exp\left(-b \cdot ADC\right) \quad [1]$$

where Sb and S0 are the signal intensities in the diffusion gradient factors of b and 0, respectively. With b-values being 0 and 1,000 s/mm^2, ADC can be calculated by fitting the signal to this model and the exponential ADC (eADC) is calculated using the formula:

$$Sb / S0 = exponential\ ADC = exp\ [-(b \times ADC)] \quad [2]$$

DKI parameters, including MD and MK, are achieved with the following Eq. [1]:

$$Sb / S0 = exp\ (-b \cdot MD + b^2 \cdot MD^2 \cdot MK / 6) \quad [3]$$

where Sb and S0 are the signal intensities acquired with the diffusion gradient factors of b and 0, respectively, along with 6 b-values (b=0, 400, 800, 1,000, 1,200, and 1,600 s/mm^2). MD is the mean diffusivity representing the corrected ADC, MK is the diffusion kurtosis.

The IVIM bi-exponential model is expressed as [2,3]:

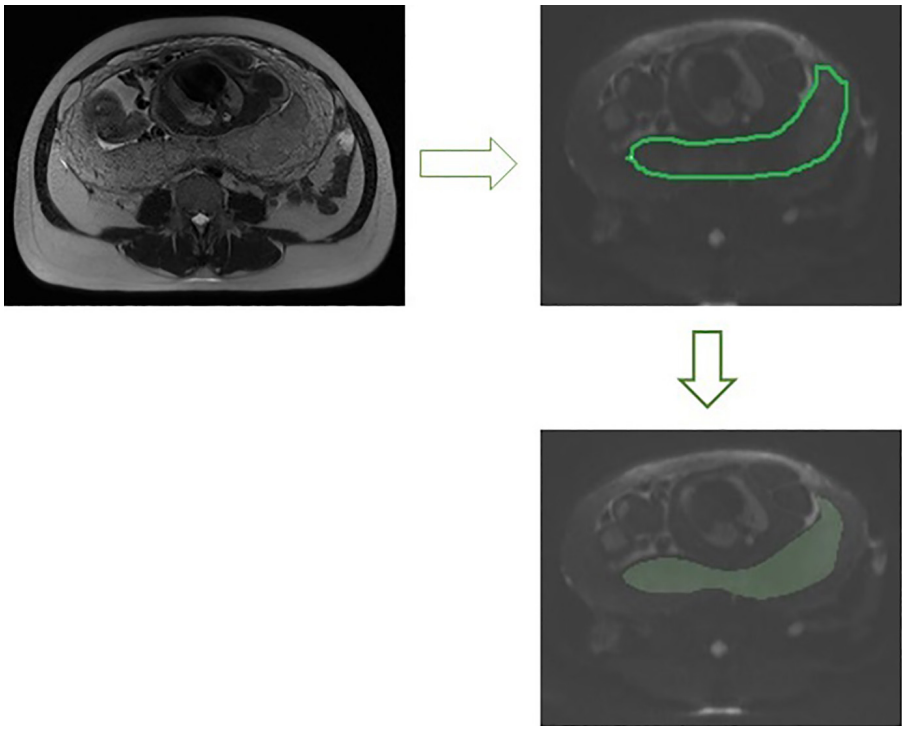

Figure 2 ROI of one slice of the placenta. ROI, region of interest.

$$Sb / S0 = (1 - f)\ exp(-b \cdot D) + f\ exp[-b \cdot (D + D^*)] \quad [4]$$

where Sb and S0 are the signal intensities in the diffusion gradient factors of b and 0, respectively. By fitting MR signal acquired at 8 b-values (b=0, 50, 100, 150, 200, 400, 600, 800 s/mm^2), the IVIM parameters, including f, D and D*, can be derived from the model. f is the perfusion fraction, D is the diffusion coefficient, and D* is the pseudo-diffusion coefficient representing pure molecular diffusion and incoherent microcirculation within the voxel, respectively.

The ADC, eADC, IVIM parameters and DKI parameters were measured with research software IMAgenGINE (Vusion Tech) (31). Two observers with 3 and 10 years, respectively, of experience in obstetric imaging independently carried out the measurement of the whole placenta. *Figure 2* shows the region of interest (ROI) of one slice of the placenta. The volume of the placenta, the mean, minimum and maximum ADC (ADC mean, ADC min, and ADC max), eADC (eADC mean, eADC min, and eADC max), MD (MD mean, MD min, and MD max), MK (MK mean, MK min, and MK max), D (D mean, D min, and D max), D* (D* mean, D* min, and D* max) and f (f mean, f min, and f max) values were automatically calculated using all slices of the DWI images covering the whole placenta. MRI scans of the DWI, ADC, eADC, f, D*, D, MD, and MK maps were also automatically produced (*Figure 3*). The inter-reader reproducibility was calculated from the measurements made by the two readers and the measurements were averaged for statistical analysis.

Statistical analysis

Depending on the distribution of variables, the parameters of the placenta from standard DWI, DKI, and IVIM are presented either as mean ± standard deviation or median and the interquartile range. The inter-reader reproducibility for parameter measurements was evaluated using the intraclass correlation coefficient (ICC) with 95% confidence intervals (CIs). An ICC <0.20 indicated slight reproducibility, between 0.21 and 0.40 indicated fair, between 0.41 and 0.60 indicated moderate, between 0.61 and 0.80 indicated substantial, and between 0.81 and 1.00 indicated perfect reproducibility. Spearman correlations were used to characterize the correlations between the parameters of standard DWI, DKI, and IVIM and gestational week and volume of the placenta. A correlation coefficient rho (r) of ≤0.24 was deemed as indicating little

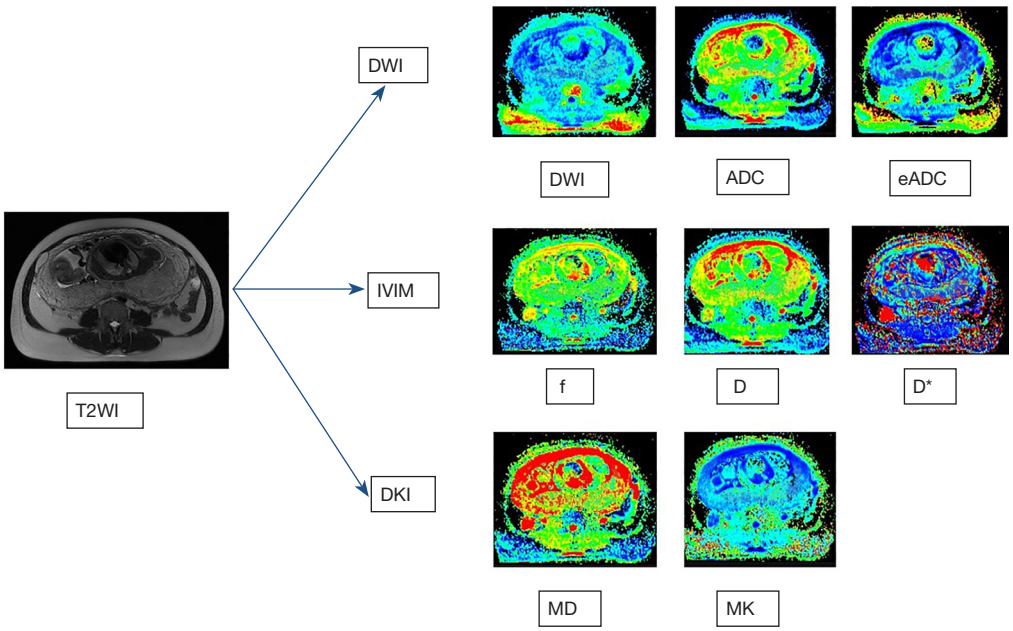

Figure 3 Diffusion weighted images of the placenta in a 37-week-old gestation woman. T2WI, T2 weighted imaging; DWI, diffusion-weighted imaging; IVIM, intravoxel incoherent motion MR imaging; DKI, diffusion kurtosis imaging; ADC, apparent diffusion coefficient; eADC, exponential ADC; f, perfusion fraction; D, pure diffusion coefficient; D*, pseudo-diffusion coefficient; MD, diffusion coefficient; MK, diffusion kurtosis.

or no correlation; 0.25–0.49, fair correlation; 0.50–0.74, moderate to good correlation; and 0.75–1.00 very good to excellent correlation; P values <0.05 were statistically significant. All analyses were performed with SPSS 21.0.

Results

Population characteristics

A total of 24 pregnant women with satisfactory images remained in the analysis. The mean maternal age was 30.09±4.17 years (range, 22–37 years), and the mean GA at examination was 31.64±4.33 weeks (range, 24–38 weeks). All medical records were received postpartum. Nine patients had placenta previa. The method of delivery included 21 cases of cesarean delivery and 3 cases of vaginal delivery.

Diffusion metrics

Table 1 shows the inter-reader reproducibility for the DWI, DKI, IVIM parameters, and the whole placenta volume. Overall, the interobserver agreement between readers was good for the whole placenta volumetric analysis. The agreement on diffusion parameters was perfect for ADC mean, ADC min, ADC max, eADC mean, eADC min, eADC max, MD mean, MK mean, f mean, D mean, D min, D max, D* mean, D* min and volume of the whole placenta. The agreement on MD min, MD max, and MK max was substantial between two observers. The average value of the two measurements was used for further analyses.

The ADC mean of the placenta was 1.51 (0.12) $\times10^{-3}$ mm^2/s, ADC min was (0.39±0.23)$\times10^{-3}$ mm^2/s, ADC max was (2.52±0.17)$\times10^{-3}$ mm^2/s, eADC mean of the placenta was 1.51 (0.12), eADC min was 0.02±0.00, eADC max was 0.57±0.20, MK mean was 0.55 (0.05), MK min was 0, MK max was 1.97±1.63, MD mean was (2.93±0.30)$\times10^{-3}$ mm^2/s, MD min was (0.06±0.43)$\times10^{-3}$ mm^2/s, MD max was (1.07±0.39) $\times10^{-3}$ mm^2/s, f mean was 0.41±0.39, f min was 0 and f max was 1, D mean was 1.57 (0.14)$\times10^{-3}$ mm^2/s, D min was (0.44±0.35)$\times10^{-3}$ mm^2/s, D max as (2.53±0.19)$\times10^{-3}$ mm^2/s, D* mean was (32.65±7.56)$\times10^{-3}$ mm^2/s, D* min was 0 and D* max was 100$\times10^{-3}$ mm^2/s.

Table 2 shows the correlations between the quantitative MR parameters, the volume of the whole placenta, and the gestational week in the normal placenta. The eADC mean, eADC max, MK mean, MK max values and volume of the whole placenta positively correlated with the gestational

Table 1 Inter-reader reproducibility for DWI, DKI, IVIM parameters and volume of the whole placenta

Parameters	ICC (95% CI)	P value
Standard DWI parameters		
ADC mean (×10^{-3} mm^2/s)	0.988 (0.955–0.997)	0.000
ADC min (×10^{-3} mm^2/s)	0.842 (0.505–0.958)	0.001
ADC max (×10^{-3} mm^2/s)	0.903 (0.664–0.975)	0.000
eADC mean	0.991 (0.965–0.998)	0.000
eADC min	0.844 (0.504–0.959)	0.001
eADC max	0.964 (0.870–0.991)	0.000
DKI parameters		
MD mean (×10^{-3} mm^2/s)	0.870 (0.562–0.966)	0.000
MD min (×10^{-3} mm^2/s)	0.751 (0.249–0.932)	0.005
MD max (×10^{-3} mm^2/s)	0.767 (0.341–0.935)	0.002
MK mean	0.991 (0.965–0.998)	0.000
MK min	N/A	N/A
MK max	0.790 (0.383–0.958)	0.002
IVIM parameters		
f mean (%)	0.896 (0.647–0.973)	0.000
f min (%)	N/A	N/A
f max (%)	N/A	N/A
D mean (×10^{-3} mm^2/s)	0.980 (0.924–0.995))	0.000
D min (×10^{-3} mm^2/s)	0.892 (0.639–0.972)	0.000
D max (×10^{-3} mm^2/s)	0.950 (0.822–0.987)	0.000
D* mean (×10^{-3} mm^2/s)	0.832 (0.454–0.956)	0.000
D* min (×10^{-3} mm^2/s)	0.990 (0.962–0.998)	0.000
D* max (×10^{-3} mm^2/s)	N/A	N/A
Volume (mL)	0.953 (0.831–0.956)	0.000

DWI, diffusion-weighted imaging; DKI, diffusion kurtosis imaging; IVIM, intravoxel incoherent motion MR imaging; ICC, intraclass correlation coefficient; CI, confidence interval; ADC, apparent diffusion coefficient; eADC, exponential ADC; MD, diffusion coefficient; MK, diffusion kurtosis; f, perfusion fraction; D, pure diffusion coefficient; D*, pseudo-diffusion coefficient.

Table 2 Correlation between quantitative MRI parameters, volume of the whole placenta and the gestational week in the normal placenta

Parameters	Gestational weeks	
	r (95% CI)	P value
Standard DWI parameters		
ADC mean (×10^{-3} mm^2/s)	–0.508 (–0.787 to 0.074)	0.016
ADC min (×10^{-3} mm^2/s)	–0.548 (–0.816 to 0.061)	0.008
ADC max (×10^{-3} mm^2/s)	0.048 (–0.323 to 0.339)	0.833
eADC mean	0.565 (–0.085 to 0.846)	0.006
eADC min	0.252 (–0.528 to 0.141)	0.258
eADC max	0.460 (0.055 to 0.747)	0.031
DKI parameters		
MD mean (×10^{-3} mm^2/s)	–0.195 (–0.601 to 0.254)	0.362
MD min (×10^{-3} mm^2/s)	–0.673 (–0.874 to 0.438)	0.001
MD max (×10^{-3} mm^2/s)	–0.236 (–0.546 to 0.255)	0. 291
MK mean	0.524 (0.069 to 0.807)	0.012
MK min	N/A	N/A
MK max	0.801 (0.504 to 0.928)	0.008
IVIM parameters		
f mean (%)	0.103 (–0.310 to 0.399)	0.650
f min (%)	–0.328 (–0.602 to 0.260)	0.136
f max (%)	N/A	N/A
D mean (×10^{-3} mm^2/s)	–0.552 (–0.828 to 0.144))	0.008
D min (×10^{-3} mm^2/s)	–0.697 (–0.873 to 4.238)	0.000
D max (×10^{-3} mm^2/s)	–0.167 (–0.509 to 0.20)	0.457
D* mean (×10^{-3} mm^2/s)	0.147 (–0.451 to 0.498)	0.515
D* min (×10^{-3} mm^2/s)	–0.594 (–0.811 to 0.239)	0.004
D* max (×10^{-3} mm^2/s)	N/A	N/A
Volume (mL)	0.566 (0.149 to 0.834)	0.006

MRI, magnetic resonance imaging; CI, confidence interval; DWI, diffusion-weighted imaging; ADC, apparent diffusion coefficient; eADC, exponential ADC; DKI, diffusion kurtosis imaging; MD, diffusion coefficient; MK, diffusion kurtosis; IVIM, intravoxel incoherent motion MR imaging; f, perfusion fraction; D, pure diffusion coefficient; D*, pseudo-diffusion coefficient.

week (r=0.565, 0.460, 0.524,0.801 and 0.566, respectively; all P<0.05), whereas the ADC mean, ADC min, MD min, D mean, D min and D* min values negatively correlated with gestational week (r=–0.508, –0.548, –0.673, –0.552, –0.697 and –0.594, respectively; all P<0.05).

Table 3 shows the correlations between the quantitative MR parameters and the volume of the whole placenta. The f mean and MK max positively correlated with the volume of the whole placenta (r=0.509 and 0.518, respectively; all P<0.05).

Table 3 Correlation between quantitative MRI parameters and volume of the whole placenta

Parameters	Volume	
	r (95% CI)	P value
Standard DWI parameters		
ADC mean (×10^{-3} mm^2/s)	–0.156 (–0.592 to 0.347)	0.488
ADC min (×10^{-3} mm^2/s)	–0.231 (–0.619 to 0.304)	0.301
ADCmax (×10^{-3} mm^2/s)	–0.141 (–0.562 to 0.193)	0.533
eADC mean	0.171 (–0.328 to 0.592)	0.446
eADC min	–0.111 (–0.507 to 0.315)	0.622
eADC max	0.254 (0.249 to 0.682)	0.255
DKI parameters		
MD mean (×10^{-3} mm^2/s)	0.266 (–0.187 to 0.658)	0.232
MD min (×10^{-3} mm^2/s)	–0.343 (–0.681 to 0.129)	0.118
MD max (×10^{-3} mm^2/s)	0.105 (–0.376 to 0.539)	0. 642
MK mean	0.250 (–0.238 to 0.645)	0.261
MK min	N/A	N/A
MK max	0.518 (0.1 to 0. 8)	0.014
IVIM parameters		
f mean (%)	0.509 (0.046 to 0.774)	0.015
f min (%)	–0.292 (–0.598 to 0.119)	0.187
f max (%)	N/A	N/A
D mean (×10^{-3} mm^2/s)	–0.168 (–0.598 to 0.321))	0.456
D min (×10^{-3} mm^2/s)	–0.377 (–0.734 to 0.085)	0.084
D max (×10^{-3} mm^2/s)	–0.220 (–0.604 to 0.234)	0.326
D* mean (×10^{-3} mm^2/s)	–0.325 (–0.701 to 0.163)	0.140
D* min (×10^{-3} mm^2/s)	–0.198 (–0.609 to 0.368)	0.378
D* max (×10^{-3} mm^2/s)	N/A	N/A

MRI, magnetic resonance imaging; CI, confidence interval; DWI, diffusion-weighted imaging; ADC, apparent diffusion coefficient; eADC, exponential ADC; DKI, diffusion kurtosis imaging; MD, diffusion coefficient; MK, diffusion kurtosis; IVIM, intravoxel incoherent motion MR imaging; f, perfusion fraction; D, pure diffusion coefficient; D*, pseudo-diffusion coefficient.

Discussion

The human placenta grows fast and undergoes structural and functional changes during pregnancy. This study aimed to explore the microstructural complexity, water diffusion, and vascular perfusion of the placenta during pregnancy using the potential of ADC, eADC, MD, MK, f, D, and D* from different DWI models.

In most of the previous studies, IVIM parameters were usually measured on a representative section of the placenta from manually placed ROIs (32-35), which may cause interobserver variability in ROI selection and inaccurate reflection of the placenta's physiological features due to inappropriate ROI selection. We adopted whole placenta volumetric analysis to assess the parameters from different DWI models of the entire placenta to avoid subjective ROI placement, ensure accuracy and repeatability of the calculation, and potentially eliminate sampling bias during data processing. The interobserver agreement was excellent between two reviewers for all the parameters. Therefore, the VOI (volume of interest)-based estimation of DWI parameters was highly reproducible and repeatable.

The negative correlation between ADC (ADC mean and ADC min) and gestational week in patients was similar to the findings of Capuani *et al.* (32). The decrease of ADC with the increase in GA might be due to calcium deposition and fibrosis, leading to barriers to diffusion, which usually occur with the maturation of the placenta, especially during the last gestational weeks (36). Our results demonstrated that D (D mean and D min) and MD (MD min) inversely correlated with increased GA. MD derived from DKI was a corrected ADC value, reflecting water molecular diffusion with non-Gaussian diffusion behavior, which had a similar meaning to ADC derived from the mono-exponential model. Meanwhile, D derived from IVIM was a pure molecular diffusion coefficient without microcapillary perfusion influence. Therefore, it is reasonable to find a negative correlation simultaneously between diffusion-related parameters and GA. As the fibrotic environment of the placenta developed during the last gestational weeks, the ADC min will decrease with the increase in GA. The ADC min showed a lower ADC value for certain placental regions containing calcium deposits and fibrotic tissue. D min and MD min decreased in the same way as ADC min. The D min value with the highest r among all the above parameters negatively correlated with GA, indicating that the D min value could be a promising parameter for depicting the maturity of the placenta.

A negative correlation between D* min and the gestational week was found in this study. D* is a perfusion-related parameter that reflects blood movement in the intervillous spaces and fetal capillaries within the villi (22). D* min represents the lower D* value in certain placental regions with calcification and fibrosis and decreased blood

movement. Therefore, blood movement decreased in such areas as the placenta matured with GA.

A positive correlation between eADC (eADC mean and eADC max), MK (MK mean and MK max), and gestational week was found in this study. eADC is another DWI parameter to avoid the T2 shine-through effect (37). The area with more diffusion restriction, such as from calcium deposits and fibrosis, might show a relative hyperintensity (high eADC value) compared with an adjacent area with less diffusion restriction (low eADC value) on the eADC map. Therefore, the eADC (eADC mean and eADC max) value positively correlated with GA, while the ADC (ADC mean and ADC min) value negatively correlated with GA.

The placenta with closely packed and extensively branched villous structures comprises the chorionic plate, chorionic basal plate, and the intervillous spaces. The development of the placental villous tree is a continuous process from primary villi to mature terminal villi characterized by elongated unbranched capillaries (2). The terminal villi formation occurs exponentially in the third trimester to ensure sufficient surface area for gas and nutrient exchange. The MK from DKI quantifies the deviation of water molecule diffusion following a Gaussian distribution and indirectly reflects the complexity of the microstructure and heterogeneity of the tissue. The greater the MK value the greater tissue complexity. In a healthy placenta, the MK value represents the complexity of the tissue within the placenta, and the MK max represents the higher MK value from certain placental regions with more complex and restricted tissue structure. Therefore, the MK value increases with GA as the placental villi grow. The MK max value with the highest r positively correlated with GA, indicating that the MK max value could be a promising parameter for evaluating the tissue complexity of the placenta.

The IVIM is a bi-exponential model that describes microscale translational movement within imaging voxels with f, representing the relative amount of blood flow in the vascular bed (34). The mean placental perfusion fraction was 41%, similar to the research of Siauve *et al.* (42.5%) (38), but higher than in other previous reports (21-23,26,31,34). Controversy remains whether the perfusion fraction is stable during gestation or whether it increases or decreases (26,32,33,38). Our results showed that the perfusion fraction did not correlate with GA, which was consistent with the studies of Siauve *et al.* (38) and Derwig *et al.* (26), but positively correlated with the volume of the whole placenta. The number and surface area of the placental villi increase with placental volume growth. Thus, the blood flow within the placenta also increases with the growth of the placental vascular bed, resulting in a higher perfusion fraction.

The deviation of tissue water molecule diffusion was measured with MK from a Gaussian distribution, which typically implied a more complex tissue microstructure. The positive correlation between MK max and the volume of the placenta might be due to the changes in the spatial arrangement and dimensions of the placental vessels with the growth of capillaries in the placenta. Therefore, the MK max value could be used as a parameter to demonstrate the complicated formation of terminal villi characterized by looping and coiling capillaries.

As the placenta grows and matures, the diffusion, perfusion, and heterogeneity of the placenta change accordingly. The hybrid IVIM-DKI model can be used to simultaneously evaluate placental function. However, our study still had some limitations. Firstly, the power of statistical analysis may be limited by the small number of participants with a normal placenta. However, this study could be considered as preliminary for future study with larger sample sizes. Secondly, the hybrid IVIM-DKI model was acquired under free-breathing, resulting in decreased signal-to-noise ratio on parameter maps. It was impossible to perform breath-hold imaging of pregnant women, so the free-breathing protocol in this study was utilized. The good reproducibility of results confirmed the reliability of measurements. Thirdly, the maximum b value utilized in this study was 1,600 s/mm^2, which is smaller than the 2,000 s/mm^2 recommended for rectal, renal, and hepatic lesions (13,14,39). With higher b-values, the effects of the restricted diffusion and superiority of the DKI model over the simple ME model can be elucidated and highlighted. However, in the clinical setting, higher b-values could lead to relatively low SNR (signal-to-noise ratio) of the images and decreased accuracy of the fitting equation. Previous abdominal DKI study has indicated that at least three b-values and three directions applied to each b value with a maximum optimal range of 1,500–2,000 s/mm^2 are appropriate for the DKI sequence (10). In this study, 11 b-values in the range of 0 to 1,600 s/mm^2 in three orthogonal directions were adopted in the DKI sequence. It is feasible to use this hybrid IVIM-DKI model in placental imaging because the protocol in this study showed satisfactory overall imaging quality with perfect interobserver agreement. Future investigation using this hybrid model might examine the functional changes

in PAS disorders, intrauterine growth restriction and preeclampsia.

In conclusion, this preliminary study showed that the D min value could depict the maturing of the placenta with increasing GA, and MK max can depict the greater tissue complexity of the placenta with the increasing of both GA and volume of the placenta. The perfusion fraction stayed stable during gestation but increased with the volume of the whole placenta.

Acknowledgments

Funding: This research was supported by the Sichuan Province Science and Technology Program (2021YJ0237).

Footnote

Reporting Checklist: The authors have completed the MDAR reporting checklist. Available at https://atm.amegroups.com/article/view/10.21037/atm-22-1037/rc

Data Sharing Statement: Available at https://atm.amegroups.com/article/view/10.21037/atm-22-1037/dss

Conflicts of Interest: All authors have completed the ICMJE uniform disclosure form (available at https://atm.amegroups.com/article/view/10.21037/atm-22-1037/coif). SW is from Siemens Healthineer. The other authors have no conflicts of interest to declare.

Ethical Statement: The authors are accountable for all aspects of the work in ensuring that questions related to the accuracy or integrity of any part of the work are appropriately investigated and resolved. The study was conducted in accordance with the Declaration of Helsinki (as revised in 2013). This study was approved by the institutional review board of Sichuan Provincial People's Hospital (No. 2021-282) and written informed consent was given by all participants.

References

1. Gude NM, Roberts CT, Kalionis B, et al. Growth and function of the normal human placenta. Thromb Res 2004;114:397-407.
2. Kingdom J, Huppertz B, Seaward G, et al. Development of the placental villous tree and its consequences for fetal growth. Eur J Obstet Gynecol Reprod Biol 2000;92:35-43.
3. Melbourne A, Aughwane R, Sokolska M, et al. Separating fetal and maternal placenta circulations using multiparametric MRI. Magn Reson Med 2019;81:350-61.
4. Ludwig KD, Fain SB, Nguyen SM, et al. Perfusion of the placenta assessed using arterial spin labeling and ferumoxytol dynamic contrast enhanced magnetic resonance imaging in the rhesus macaque. Magn Reson Med 2019;81:1964-78.
5. Remus CC, Solano E, Ernst T, et al. Comparative analysis of high field MRI and histology for ex vivo whole organ imaging: assessment of placental functional morphology in a murine model. MAGMA 2019;32:197-204.
6. Flouri D, Owen D, Aughwane R, et al. Improved fetal blood oxygenation and placental estimated measurements of diffusion-weighted MRI using data-driven Bayesian modeling. Magn Reson Med 2020;83:2160-72.
7. Sannananja B, Ellermeier A, Hippe DS, et al. Utility of diffusion-weighted MR imaging in the diagnosis of placenta accreta spectrum abnormality. Abdom Radiol (NY) 2018;43:3147-56.
8. Manganaro L, Fierro F, Tomei A, et al. MRI and DWI: feasibility of DWI and ADC maps in the evaluation of placental changes during gestation. Prenat Diagn 2010;30:1178-84.
9. Sivrioğlu AK, Özcan Ü, Türk A, et al. Evaluation of the placenta with relative apparent diffusion coefficient and T2 signal intensity analysis. Diagn Interv Radiol 2013;19:495-500.
10. Rosenkrantz AB, Padhani AR, Chenevert TL, et al. Body diffusion kurtosis imaging: Basic principles, applications, and considerations for clinical practice. J Magn Reson Imaging 2015;42:1190-202.
11. Jensen JH, Helpern JA, Ramani A, et al. Diffusional kurtosis imaging: the quantification of non-gaussian water diffusion by means of magnetic resonance imaging. Magn Reson Med 2005;53:1432-40.
12. Xiao Z, Zhong Y, Tang Z, et al. Standard diffusion-weighted, diffusion kurtosis and intravoxel incoherent

motion MR imaging of sinonasal malignancies: correlations with Ki-67 proliferation status. Eur Radiol 2018;28:2923-33.
13. Cui Y, Yang X, Du X, et al. Whole-tumour diffusion kurtosis MR imaging histogram analysis of rectal adenocarcinoma: Correlation with clinical pathologic prognostic factors. Eur Radiol 2018;28:1485-94.
14. Ding Y, Tan Q, Mao W, et al. Differentiating between malignant and benign renal tumors: do IVIM and diffusion kurtosis imaging perform better than DWI? Eur Radiol 2019;29:6930-9.
15. Wan Q, Deng YS, Lei Q, et al. Differentiating between malignant and benign solid solitary pulmonary lesions: are intravoxel incoherent motion and diffusion kurtosis imaging superior to conventional diffusion-weighted imaging? Eur Radiol 2019;29:1607-15.
16. Raab P, Hattingen E, Franz K, et al. Cerebral gliomas: diffusional kurtosis imaging analysis of microstructural differences. Radiology 2010;254:876-81.
17. Hori M, Fukunaga I, Masutani Y, et al. New diffusion metrics for spondylotic myelopathy at an early clinical stage. Eur Radiol 2012;22:1797-802.
18. Wang JJ, Lin WY, Lu CS, et al. Parkinson disease: diagnostic utility of diffusion kurtosis imaging. Radiology 2011;261:210-7.
19. Le Bihan D. Intravoxel incoherent motion imaging using steady-state free precession. Magn Reson Med 1988;7:346-51.
20. Le Bihan D, Breton E, Lallemand D, et al. MR imaging of intravoxel incoherent motions: application to diffusion and perfusion in neurologic disorders. Radiology 1986;161:401-7.
21. Moore RJ, Ong SS, Tyler DJ, et al. Spiral artery blood volume in normal pregnancies and those compromised by pre-eclampsia. NMR Biomed 2008;21:376-80.
22. Moore RJ, Issa B, Tokarczuk P, et al. In vivo intravoxel incoherent motion measurements in the human placenta using echo-planar imaging at 0.5 T. Magn Reson Med 2000;43:295-302.
23. Lu T, Pu H, Li KD, et al. Can introvoxel incoherent motion MRI be used to differentiate patients with placenta accreta spectrum disorders? BMC Pregnancy Childbirth 2019;19:531.
24. Lu T, Song B, Pu H, et al. Prognosticators of intravoxel incoherent motion (IVIM) MRI for adverse maternal and neonatal clinical outcomes in patients with placenta accreta spectrum disorders. Transl Androl Urol 2020;9:258-66.
25. Alison M, Chalouhi GE, Autret G, et al. Use of intravoxel incoherent motion MR imaging to assess placental perfusion in a murine model of placental insufficiency. Invest Radiol 2013;48:17-23.
26. Derwig I, Lythgoe DJ, Barker GJ, et al. Association of placental perfusion, as assessed by magnetic resonance imaging and uterine artery Doppler ultrasound, and its relationship to pregnancy outcome. Placenta 2013;34:885-91.
27. Iima M, Kataoka M, Kanao S, et al. Intravoxel Incoherent Motion and Quantitative Non-Gaussian Diffusion MR Imaging: Evaluation of the Diagnostic and Prognostic Value of Several Markers of Malignant and Benign Breast Lesions. Radiology 2018;287:432-41.
28. Lu Y, Jansen JF, Mazaheri Y, et al. Extension of the intravoxel incoherent motion model to non-gaussian diffusion in head and neck cancer. J Magn Reson Imaging 2012;36:1088-96.
29. León RL, Li KT, Brown BP. A retrospective segmentation analysis of placental volume by magnetic resonance imaging from first trimester to term gestation. Pediatr Radiol 2018;48:1936-44.
30. Capital Institute of Pediatrics; Coordinating Study Group of Nine Cities on the Physical Growth and Development of Children. Growth standard curves of birth weight, length and head circumference of Chinese newborns of different gestation. Zhonghua Er Ke Za Zhi 2020;58:738-46.
31. Yang M, Yan Y, Wang H. IMAge/enGINE: a freely available software for rapid computation of high-dimensional quantification. Quant Imaging Med Surg 2019;9:210-8.
32. Capuani S, Guerreri M, Antonelli A, et al. Diffusion and perfusion quantified by Magnetic Resonance Imaging are markers of human placenta development in normal pregnancy. Placenta 2017;58:33-9.
33. Jakab A, Tuura RL, Kottke R, et al. Microvascular perfusion of the placenta, developing fetal liver, and lungs assessed with intravoxel incoherent motion imaging. J Magn Reson Imaging 2018;48:214-25.
34. Jakab A, Tuura R, Kottke R, Kellenberger CJ, Scheer I. Intra-voxel incoherent motion MRI of the living human foetus: technique and test-retest repeatability. Eur Radiol Exp 2017;1:26.
35. Lu T, Pu H, Cui W, et al. Use of intravoxel incoherent motion MR imaging to assess placental perfusion in patients with placental adhesion disorder on their third trimester. Clin Imaging 2019;56:135-9.
36. Baergen RN. Manual of pathology of the human placenta.

Second Edition Springer, Boston, MA, 2011.
37. Park SY, Kim CK, Park JJ, et al. Exponential apparent diffusion coefficient in evaluating prostate cancer at 3 T: preliminary experience. Br J Radiol 2016;89:20150470.
38. Siauve N, Hayot PH, Deloison B, et al. Assessment of human placental perfusion by intravoxel incoherent motion MR imaging. J Matern Fetal Neonatal Med 2019;32:293-300.
39. Cao L, Chen J, Duan T, et al. Diffusion kurtosis imaging (DKI) of hepatocellular carcinoma: correlation with microvascular invasion and histologic grade. Quant Imaging Med Surg 2019;9:590-602.

(English Language Editor: K. Brown)

Cite this article as: Lu T, Wang Y, Guo A, Wei C, Chen Y, Wang S, Song B. Standard diffusion-weighted, diffusion kurtosis and intravoxel incoherent motion MR imaging of the whole placenta: a pilot study of volumetric analysis. Ann Transl Med 2022;10(6):269. doi: 10.21037/atm-22-1037

